



The Behavior of Enlarged Base Pile Under Compression and Uplift Loading in Partially Saturated Sand

Zaid H. Ghalib^{1*} , Mahmood R. Mahmood¹

¹ Department of Civil Engineering, University of Technology, Baghdad, Iraq.

Received 03 June 2024; Revised 15 September 2024; Accepted 24 September 2024; Published 01 October 2024

Abstract

The aim of this paper is to study the behavior of enlarged base piles embedded within partially saturated soils under compression and uplift loading. This type of pile is rarely excavated and cast on-site. Accordingly, to construct an enlarged base pile model, an excavator was designed and manufactured to give appropriate shape through drilling and casting in the laboratory through the design and manufacture of an excavator to produce piles with a shaft of 35 mm in diameter, 500 mm in length, and a base of 80 mm in diameter inclined at an angle of 60 degrees. Three different partial saturation soils were achieved by lowering the water level below the soil surface 20, 40, and 60 cm and measuring the suction force of each stage using a Tensiometer. The average matrix suction results were 6.4, 7.6, and 9.1 kPa for each lower water level, respectively. The test results showed that the bearing capacity of the enlarged base piles under compression load in partially saturated soil was higher than that in the case of full saturation because of matrix suction, with an improvement rate of 2.5–4.5 times compared with the case of fully saturated soil. Additionally, test results showed that the enlarged base piles subjected to uplift loading in partially saturated soil were significantly improved compared with the fully saturated condition, with an improvement rate of 1.5 - 3 times. The reason for this is the apparent surface cohesion of the sandy soil, which increases the bearing capacity of the sandy soil. This study sheds light on the phenomenon of apparent surface cohesion of sandy soil and the extent of its effect on increasing the soil's resistance to the loads placed on it.

Keywords: Enlarged Base Pile; Partially Saturated Soil; Matric Suction; Apparent Cohesion; SWCC; Uplift.

1. Introduction

Enlarged base pier (belled pier) foundations have been shown to be affordable for transmission line towers with narrow high-rise structures, as they can withstand significant uplift loads. They offer resistance against both lift and compression [1]. When the hard layer is extremely far or not found, the bearing resistance is neglected in this case, and the pile may be pulled out due to the uplift force. To solve this problem, the designers suggest the friction pile be increased in length or diameter or both length and diameter. Still, increasing the pile's dimensions is sometimes ineffective and costly. Belled piers, or enlarged base piles, are an economic foundation style that can withstand both compressive and uplift loads [2].

Recently, many cities have used larger foundation piles to support various constructions in various soil types, such as buildings, bridges, and industrial operations. In other words, tall buildings subject to wind force and seismic action use this type of pile, and it is assumed that the maximum resistance to uplift fits into a bell angle [3]. When groundwater levels are high, uplifting can also happen on sandy soil. Additionally, in sandy soil with cavities, embedded and belled piles can be used [4]. The bells boost the bearing capacity of the piles under pull-out and compressive loadings by distributing the loads across the soil [5].

* Corresponding author: bce.23.68@grad.uotechnology.edu.iq

 <http://dx.doi.org/10.28991/CEJ-2024-010-10-08>



© 2024 by the authors. Licensee C.E.J, Tehran, Iran. This article is an open access article distributed under the terms and conditions of the Creative Commons Attribution (CC-BY) license (<http://creativecommons.org/licenses/by/4.0/>).

However, evaluating the ultimate compressive and uplift capacity of enlarged base piles and determining the failure surface's position is still a concern in geotechnical engineering. The pile-soil interaction mechanism is poorly understood, and only very little literature is available to analyze the ultimate uplift and compressive capacity and failure mechanism. Conventional soil mechanics techniques have been applied in geotechnical engineering to construct pile foundations assuming the soil is saturated. However, natural soils are often unsaturated because the water table is intense. Many geotechnical constructions, such as heavy structures and dams, are constructed on compressed, unsaturated soils that are strong enough to support foundations [6].

Locating shallow and deep foundations above the water table, where the soil is unsaturated, is best to sustain loads from superstructures [7]. Higher carrying capacity can be achieved by distributing the pressures these foundations create over the unsaturated soil layer above the water table. Conventional shallow and deep foundation design typically ignores the impact of capillary pressures, or matric suction, in this area. Dismissing the impact of capillary pressures on unsaturated soil's bearing capacity would be equivalent to dismissing the significance of reinforcement in the design of reinforced concrete structures [8]. Some studies demonstrated how matric suction affects unsaturated soils' carrying capacity [8-10]. The impact of matric suction on the design of various foundation types has been the subject of several research studies that have been published in the literature [11-13].

2. Test Setup

The steel frame, steel soil tank, and enlarged base pile configuration depicted in the plate (1) were used for all model tests, and the model piles were subjected to a vertical load using a five-ton capacity compression electrical jack. Throughout all the experimental testing, the loading rate remains roughly constant 3-ton capacity load cell is used to measure the applied load. Three-channel data loggers and LabVIEW serve as the representation of the data acquisition device. For testing, graphical programming is employed. The vertical movement of the pile is measured using a computerized linear variable differential transducer (LVDT) for monotonic movement (model KTR-50 mm) to calculate the pile's displacements. Three Tensiometers were used to monitor the soil's matric suction (see Figures 1 and 2).



Figure 1. Experimental model

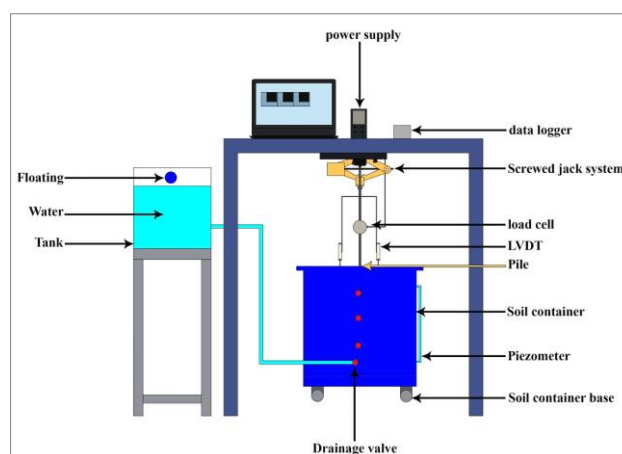


Figure 2. Schematic diagram of the experimental model

2.1. Description of the Soil Used

Dry sand was used in this investigation, which was taken from the Iraq Gate Project’s location in Baghdad city. These typical examinations are run to ascertain the physical characteristics of the soil used:

1. Direct shear test.
2. Maximum and minimum dry unit weight.
3. Grain size distribution.
4. Specific gravity.

Figure 3 presents grain size distribution for the sand used, and Table 1 shows the testing result.

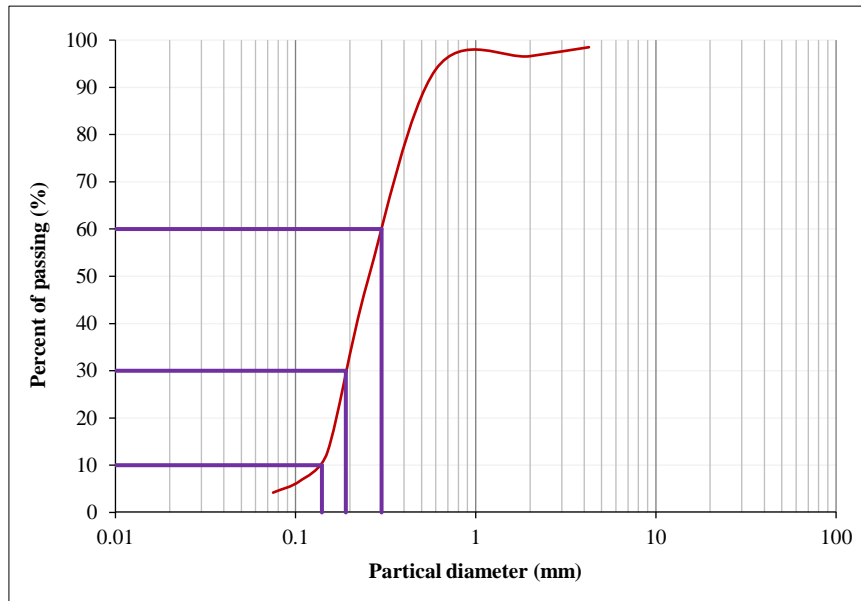


Figure 3. Grain Size Distribution

Table 1. Physical properties of the sand used in present tests

Index property	Value	Standers
Specific gravity (Gs)	2.63	ASTM D 854-06 [14]
D10 mm	0.14	
D30 mm	0.195	
D60 mm	0.31	
Cu	2.38	
Cc	0.94	
Soil classification, USCS	SP	ASTM D422-00 [15]
Max. dry unit weight (kN/m ³)	16.8	ASTM D4253 [16]
Min. dry unit weight (kN/m ³)	13.6	ASTM D4254 [17]
Relative density, RD (%)	50%	
The angle of internal friction ϕ for dry sand (degree)	35	ASTM D 3080-90 [18]
The angle of internal friction ϕ for fully saturated sand (degree)	28	ASTM D 3080-90 [18]

2.2. Enlarged Base Pile Model and Excavator

Model piles were designed and manufactured from reinforced concrete with a 35 mm shaft diameter and 80 mm base diameter with 500 mm length, corresponding to (L/d) ratio of 14. These pile models were also excavated on-sand box using an excavator manufactured according to specific measurements. They consist of a tube with an outer diameter of 35 mm containing blades inclined at an angle of 60 degrees. They are opened to expand the base with a diameter of 80 mm when reaching the required depth. They were also cast on-sand box to represent reality as much as possible; Figures 4 and 5 show the excavator and the pile models.



Figure 4. Excavator



Figure 5. Pile model

3. Partially Saturated Soil

The process of making partially saturated soil will take place in three stages. After the soil is compacted inside the container according to the required relative density of 50%, the process of completely saturating the model will take place through a water supply connected to the tank from the bottom through the valve at the bottom. The soil will be left saturated with water for 24 hours to ensure 100% saturation. After this process, the water table will be lowered to 20 cm below the soil surface by opening the first valve and leaving it for 24 hours to ensure that the equilibrium condition corresponding to suction will be achieved. Three different lowering stages of the water table below the soil surface (20, 40, and 60 cm) will achieve partial saturation of soil of different soil suctions.

3.1. Soil Suction Direct Measurement (Tensiometer Method)

Tensiometer is the traditional word for a device that measures negative pore water pressures directly. A Tensiometer is made up of a fluid-filled reservoir that separates a stress measurement device from a porous filter. The fluid in the reservoir is often water; thus, Tensiometers and piezometers are comparable in terms of their component elements. They function by letting the water seep into the soil from the Tensiometer until the soil suction, or the stress keeping the water in the soil, equals the stress holding the water in the Tensiometer. If this requirement is satisfied, no more water interaction between the soil and the Tensiometer will occur. After that, a stress-measuring tool can be employed to monitor the soil suction, such as an electric pressure sensor, vacuum gauge, or manometer, as it will show up in the reservoir as tensile stress in the water. Tensiometers are used to measure negative pore water pressures as shown in Figure 6 [19].



Figure 6. Tensiometer insertion

3.2. Results of the Suction Profile Set

In this study, the matrix suction in the sand was measured using three Tensiometers positioned at various depths below the soil's surface. It needed 24 hours to reach equilibrium conditions. Three Tensiometers are used to specify the soil's suction values for the suction profile chosen. Tensiometers were positioned as follows: the first was positioned 10 cm below the soil's surface, the second 30 cm below it, and the third 50 cm below the soil surface. To achieve complete saturation and allow air to escape from the soil, the water level in the soil tank was raised from the bottom. After that, the water table was lowered for 24 hours to 20 cm below the soil's surface, as shown in Figure 7, as a first stage.

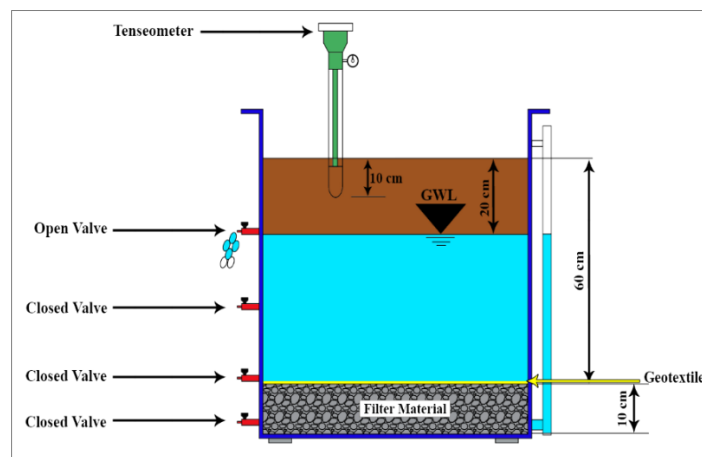


Figure 7. Profile suction of the first stage

At the second and third stages, the water level lowers below the soil surface to 40 and 60cm, respectively, as shown in Figures 8 and 9.

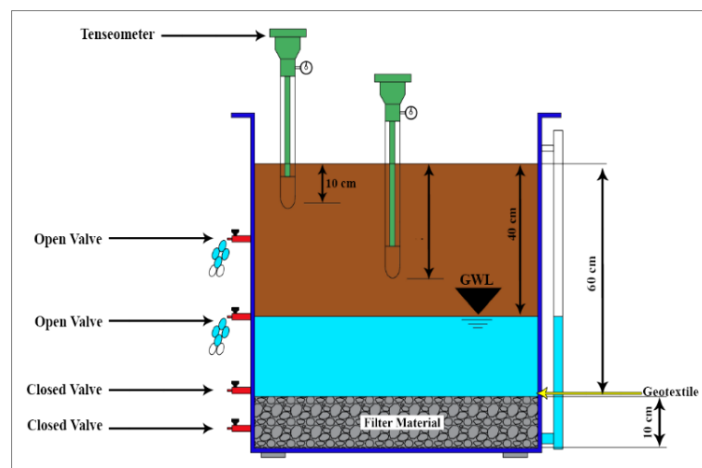


Figure 8. Profile suction of the second stage

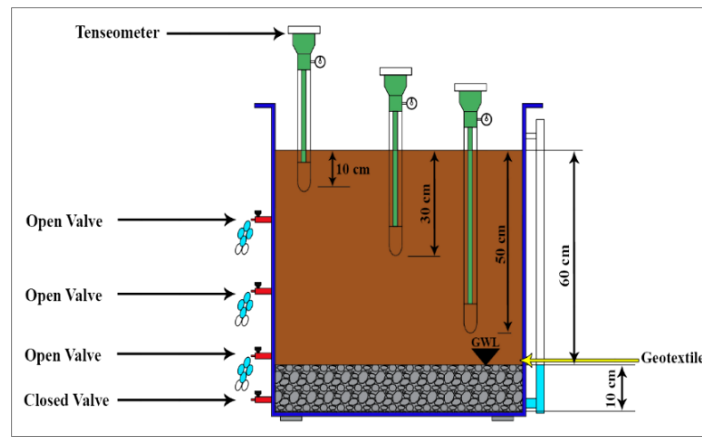


Figure 9. Profile suction of the third stage

After 24 hours, the matrix suction is measured. According to the soil's suction profile, the matrix suction increased as the water table dropped. As the water table drops, the soil suction increases sharply in the vicinity of the soil surface (10 cm below the soil surface). The high rise in matric suction values at the soil surface may be due to the evaporation of water from the soil surface [20, 21]. Figure 10 shows the relation between matrix suction and the three lowering stages of water level below the soil surface. Table 2 shows the average matrix suction results for each stage.

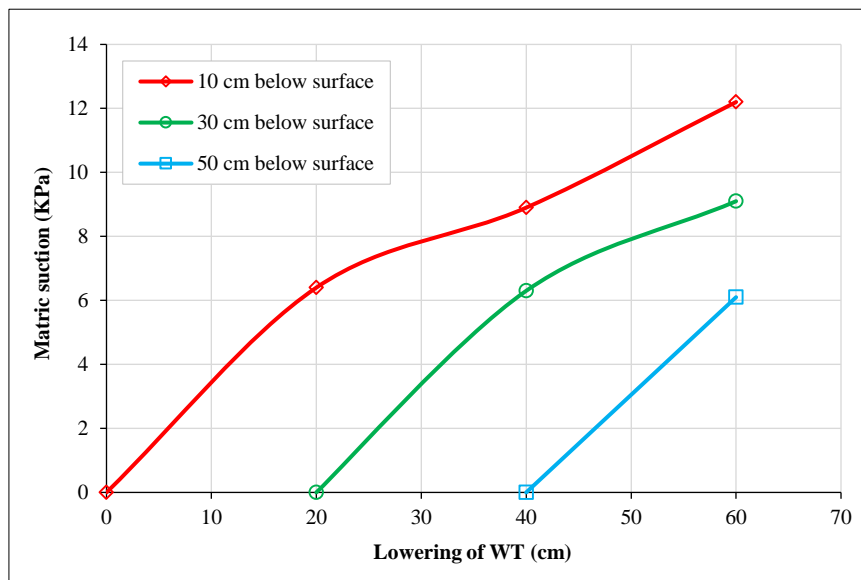


Figure 10. Matric suction values of the water table below the soil surface for all stages

Table 2. Presents an overview of the average matrix suction results correlating to reducing the water table suction profile set

Corresponding average Matric suction in (kPa)	Lowering of the water table from the soil surface in (cm)	Soil conditions
0	0	Fully saturated
6.4	20	Partially saturated
7.6	40	
9.1	60	

3.3. Soil Water Characteristic Curve (SWCC)

The relation between matric suction and water content is represented by the Soil-Water Characteristic Curve (SWCC) and is widely used to estimate unsaturated soil functions, including permeability, water storage, shear strength, and thermal property [22]. Figure 11 shows relationships between the matric suction and gravitational water content that are produced by the soil vision program utilizing the Van Genuchten equation. Figure 12 shows relationships between the matric suction and gravitational water content produced by the soil vision program utilizing the Fredlund and Xing equation.

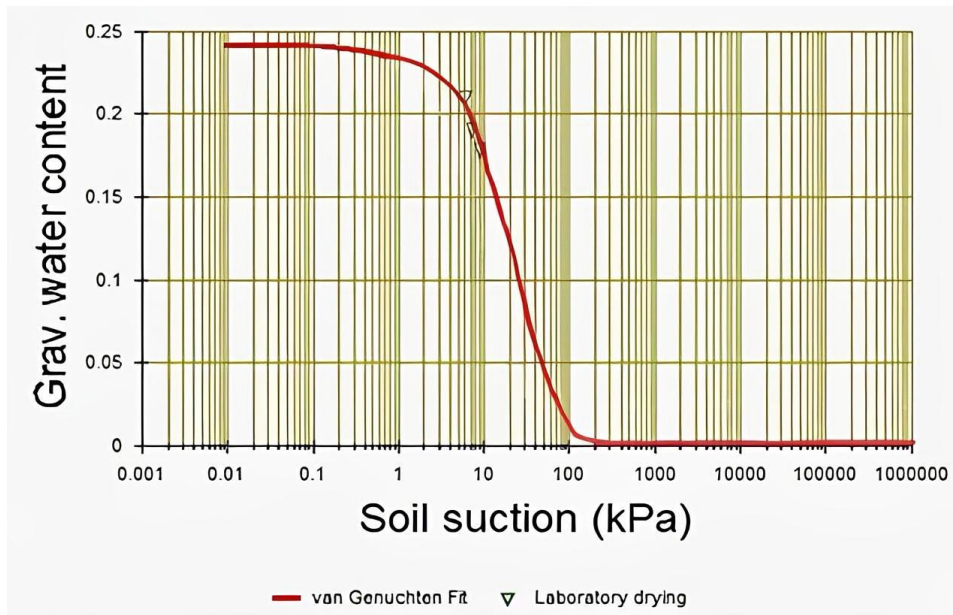


Figure 11. Relationships between the matric suction and gravitational water content that are produced by the soil vision program utilizing the Van Genuchten equation

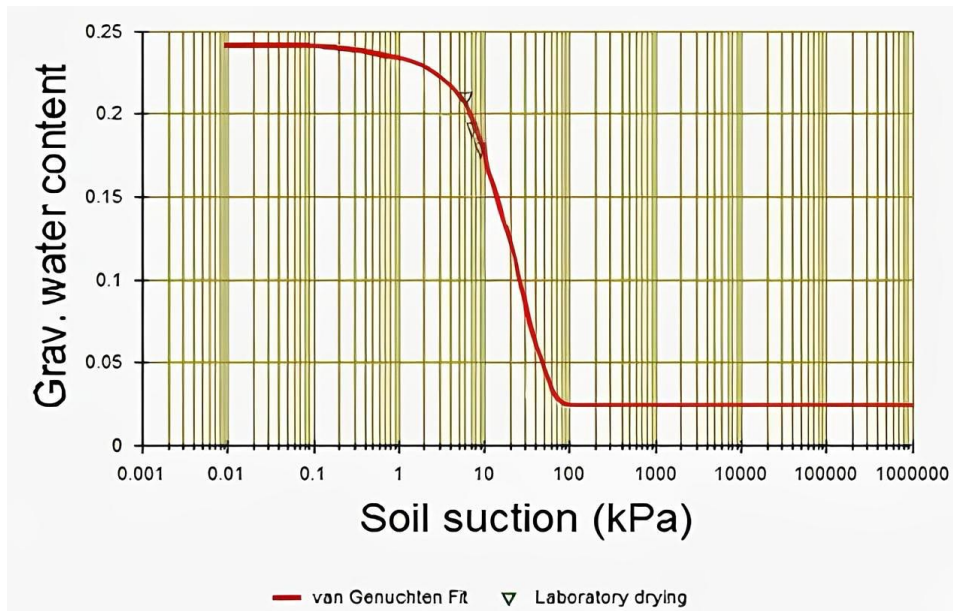


Figure 12. Relationships between the matric suction and gravitational water content produced by the soil vision program utilizing the Fredlund & Xing equation

There are two variations in slope along the soil's SWCC; the slope changes define two essential points in understanding the SWCC [22]; the biggest voids begin to desaturate at the first point, known as the soil's "air-entry value" when suction is raised. The second point, known as "residual conditions," designates the point at which it becomes noticeably harder to remove water from the soil (i.e., it takes more energy to remove water from the soil). The SWCC is divided into three separate zones according to changes in slope: the "residual zone," the "transition zone" between the air-entry value and the residual value, and the "boundary effect zone" in the lower suction range.

Based on the soil water characteristics curve, Figures 11 and 12, and fitting curves recommended by Fredlund & Xing [23] and Van Genuchten [24], the air-entry value ($u_a - u_w$) (kPa) was 3.12 and 3.24 kPa, respectively. The various parameters in each equation generally do not affect the curves' shapes; nevertheless, the parameters' values vary significantly according to how many data points are utilized to fit the curve [25]. This explains why there is no significant difference between the two curves and why there is no noticeable abrupt shift in the curves' slope. It is advised that the equation proposed by Fredlund & Xing [23] be used for the soil-water characteristic curve since it provided the greatest match among the other equations [25].

4. Apparent Surface Cohesion

The most often used strength metric in unsaturated soils that captures the impact of matric suction is apparent cohesion; however, obtaining it can be challenging. It is necessary to do an involved strength test. According to soil mechanics, the surface tension of the moisture layer enveloping each particle prevents them from separating from one another. The Equation 1 can be used to quantify apparent cohesiveness [15]:

$$C = (u_a - u_w) \times \tan\phi \times S \times \left(0.075/D_{10}\right)^2 + 5 \tag{1}$$

where: $u_a - u_w$ is Matric suction (KPa), ϕ is Angel of internal friction, S is Degree of saturation, D_{10} is the diameter of the particles of which 10% of the soil is finer (mm) (effective diameter).

5. Testing Program

This research will examine the impact of soil suction around the enlarged base piles, comparing with the dry and fully saturated cases while varying the water level in three stages 20, 40, and 60 cm for different matrix suction. Figure 13 shows a flow chart for the testing program.

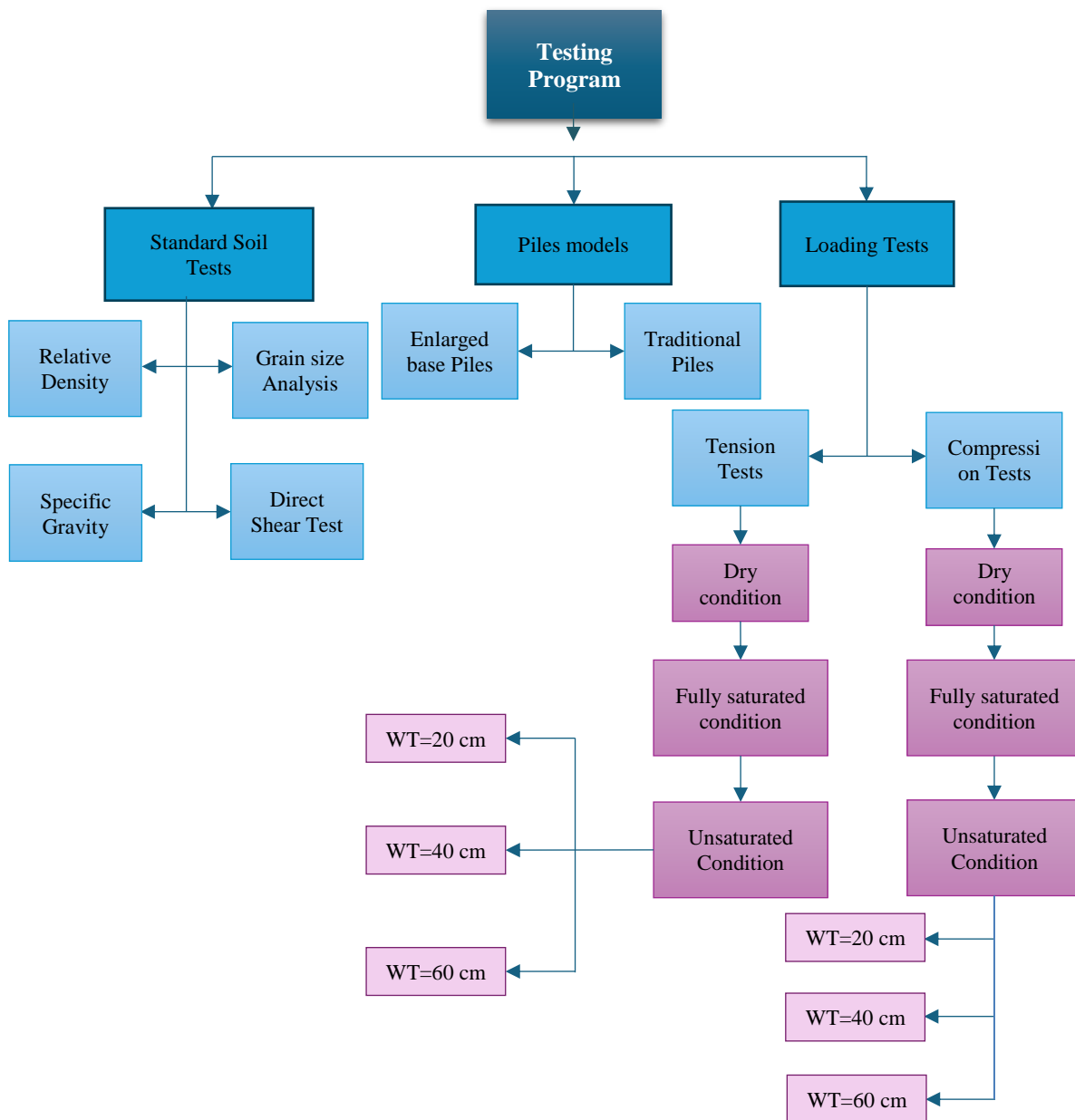


Figure 13. Flow chart for the testing program

6. Results

6.1. Load- Displacement Diagrams

A set of tests were conducted on samples of enlarged base piles that were excavated and cast on a laboratory sand tank. A vertical load was applied to the piles to test the soil's bearing capacity under uplift and compression loads. The results for partially saturated soil at different matric suction of 6.4, 7.6, and 9.1 kPa with different water levels are compared with dry and fully saturated soil, as shown in Figure 14. In this research, Terzaghi proposed [26] will be adopted to find the (Q_{ult}) that the enlarged base piles can bear through load–settlement curves. Failure is defined as the load corresponding to the displacement of 10% of the model footing width (or pile diameter).

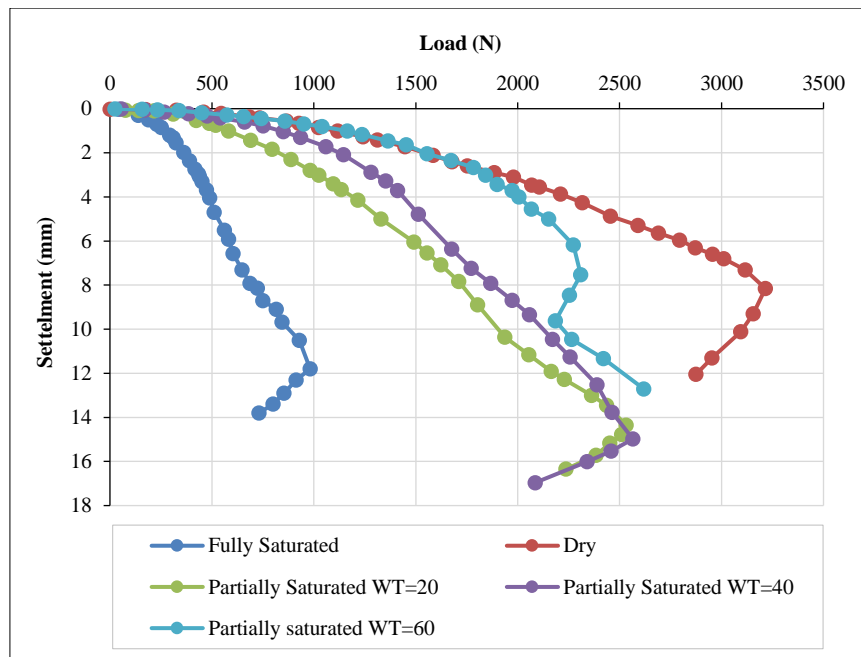


Figure 14. The load settlement curve of the enlarged base pile under compression load

Figure 14 shows the load settlement curve of the enlarged base pile under compression load. The ultimate bearing capacity in fully saturated soil gives the lowest load value of 463N, which is intuitive. However, when the water level drops to 20 cm below the soil surface, an increase in the value of the ultimate bearing capacity to 1109 N, which indicates the effect of matrix suction, which means causing the negative pore water pressure and increasing the effective stress, as the improvement ratio reaches 240% when compared to the case of full saturation. As the water level continues to decrease to 40 and 60 cm below the soil surface, there is an increase in the value of the ultimate bearing capacity by up to 1382 N and 1918 N with improvement ratios of 290% and 414%, respectively. When the maximum value of the matrix suction reached 9.1 kPa at a water table level of 60 cm below the soil surface, the ultimate bearing capacity is found to be relatively close to the dry state. The reason is that the enlarged base pile rests on partially saturated soil, as the apparent surface cohesion phenomenon occurs in partially saturated soil, where soil particles are bounded by electrical contraction, increasing the effective stress and thus increasing the shear strength coefficients of unsaturated soil. Another reason is that the increase in water content is inversely proportional to the soil's internal friction angle. This pattern of results agrees with numerous recent studies, such as [11-13, 27-29], proving that, in both fine- and coarse-grained unsaturated soils, matric suction is a significant factor in determining the bearing capacity of shallow and deep foundations.

Figure 15 shows a load-displacement curve of the enlarged base pile under uplift load; the uplift resistance in the case of full saturation also gives the lowest value of 564N, which is intuitive, but when the water level decreases to 20 cm below the soil surface, there is an increase in the ability to uplift resistance due to the effect of the matrix suction to 1077N with an improvement ratio of up to 191% compared to the fully saturated case. This results in an increase in effective stress due to the creation of negative pore water pressure; in other words, the soil, by the action of the matrix suction, works on the pile confinement. This is strongly shown when the water is reduced to 40 and 60 cm, respectively, below the soil surface, with an improvement ratio of up to 205% and 251% compared to the fully saturated case; as well, this pattern of results agrees with numerous recent studies [30, 31].

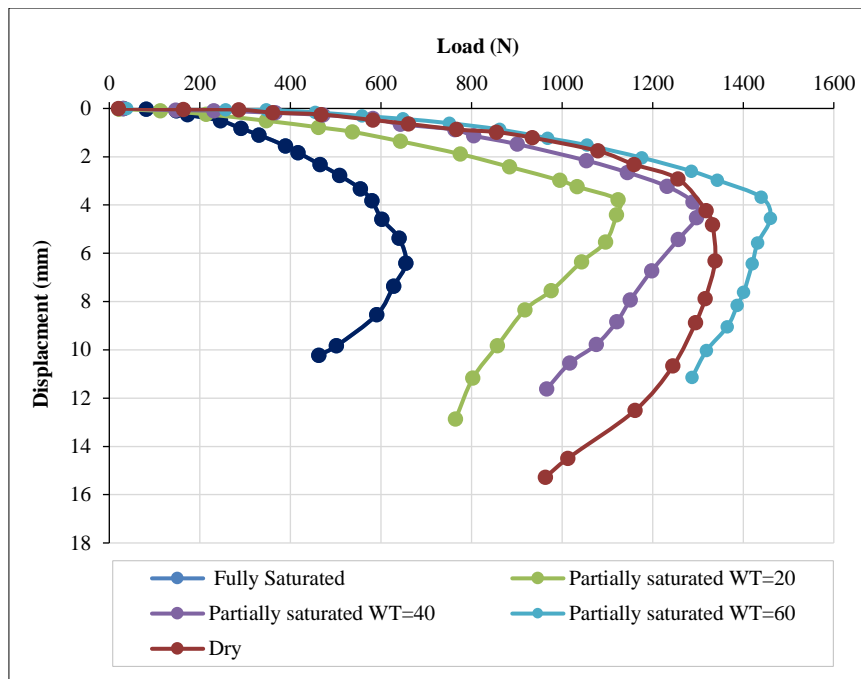


Figure 15. The load-displacement curve of the enlarged base pile under uplift load

Table 3 shows the result of ultimate compression bearing and uplift capacities of the enlarged base pile.

Table 3. Result of ultimate compression bearing and uplift capacities of the enlarged base pile

Lowering of the Water table (cm)	Average matric Suction (kPa)	Ultimate compression bearing Capacity (N)	Ultimate uplift Capacity (N)	Apparent Surface Cohesion (KPa)
0	-	463	564	-
20	6.4	1109	1077	5.8
40	7.6	1382	1155	6.03
60	9.1	1918	1416	6.23
Dry	-	2081	1284	-

6.2. Variation of Ultimate Bearing Capacity with Matric Suction for Compression and up Lift Loading

Figures 16 and 17 demonstrate the relationship of ultimate bearing capacity in compression and up lift with different values of matric suction, a notable increase in matrix suction results in an improvement in bearing capacity. Furthermore, the results show that the air entrance value (boundary impact zone) causes the final bearing capacity to rise roughly linearly with matric suction.

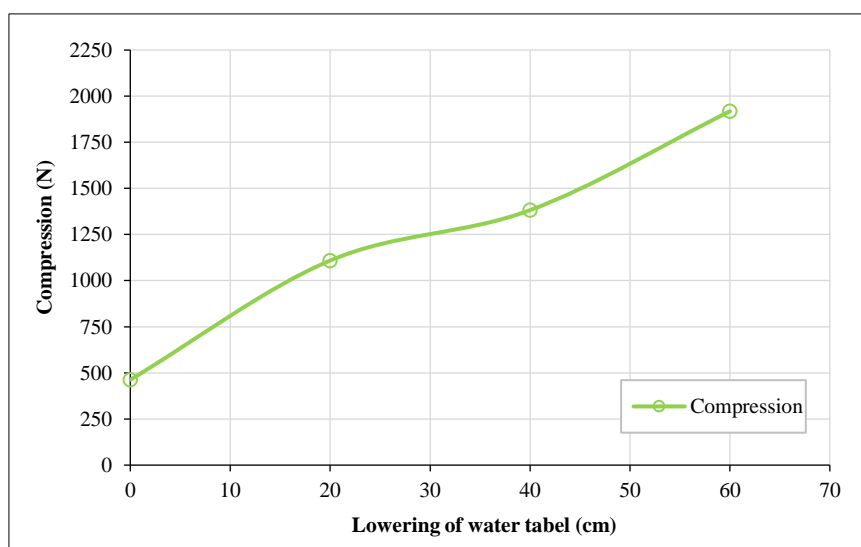


Figure 16. Variation of the ultimate bearing capacity to average matric suction for all the models

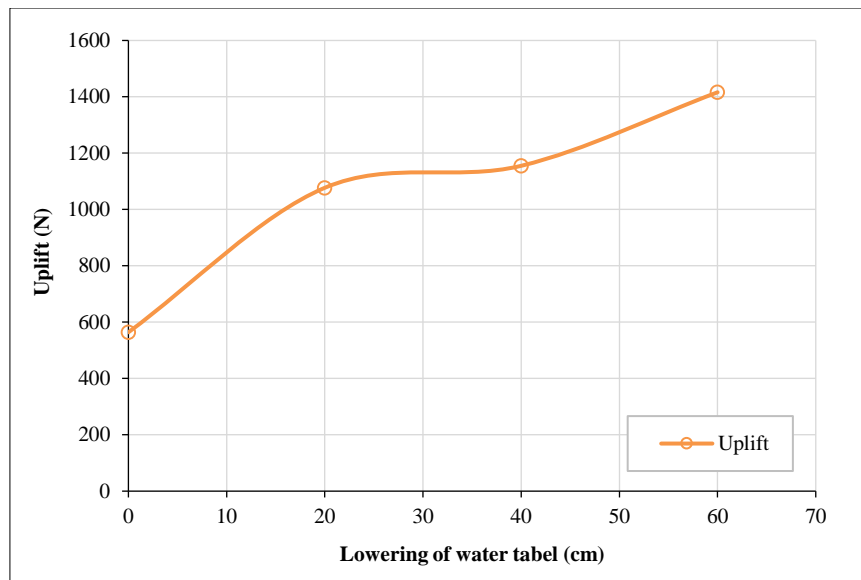


Figure 17. Variation of the ultimate uplift resistance to average matric suction for all the models

The correlation between the ultimate load capacity for all the models utilized in this investigation and the lowering of the water table from the soil surface revealed that all models have a higher load capacity as the water table drops. However, the effect of partial saturation of soil increases as the groundwater level drops. This can be explained by a rise in the overburden pressure and a rise in the matric suction value due to the expansion of the unsaturated zone.

7. Conclusion

The bearing capacity of the enlarged base piles under compressive load in partially saturated soil was higher than that in the case of full saturation because of matrix suction, with an improvement rate of 2.5–4.5 times compared to the case of full saturation. Moreover, the enlarged base piles subjected to uplift loading in partially saturated soil were significantly improved compared to the full saturation condition, with improvement rates reaching 1.5 - 3 times when compared to the fully saturated state as the matric suction makes the soil confine the pile. In addition, it was found that the soil close to the surface when the water level is lowered has a higher value of matric suction than the soil that is close to the water level; this is because the soil near the water table has a higher water content than the soil at the surface, which has a higher air content. For sandy soil, the value of the angle of internal friction decreases with increasing soil water content. It has also been proven that the phenomenon known as apparent surface cohesion, which is inversely proportional to the water content, is responsible for the rise in bearing capacity in compression and the uplift resistance to tension.

8. Declarations

8.1. Author Contributions

Conceptualization, M.R.M.; methodology, Z.H.G.; software, Z.H.G.; writing—original draft preparation, Z.H.G.; writing—review and editing, M.R.M.; supervision, M.R.M. All authors have read and agreed to the published version of the manuscript.

8.2. Data Availability Statement

The data presented in this study are available in the article.

8.3. Funding

The authors received no financial support for the research, authorship, and/or publication of this article.

8.4. Conflicts of Interest

The authors declare no conflict of interest.

9. References

- [1] Hamza, A. S. H. A. (1994). Transmission line tower representation and its effect on the tower surge response calculation. *Energy Conversion and Management*, 35(12), 1087–1096. doi:10.1016/0196-8904(94)90012-4.
- [2] Dickin, E. A., & Leung, C. F. (1992). The influence of foundation geometry on the uplift behaviour of piles with enlarged bases. *Canadian Geotechnical Journal*, 29(3), 498–505. doi:10.1139/t92-054.
- [3] Kiriya, T., Zhou, Y., & Asaka, Y. (2024). Estimation of belled pile uplift resistance in dense sand based on centrifugal experiments. *Japanese Geotechnical Society Special Publication*, 10(48), 1780–1785. doi:10.3208/jgsssp.v10.os-37-01.
- [4] Al-Mosawe, M. J., Al-Shakarchi, Y. J., & Al-Taie, S. M. (2007). Embedded in Sandy Soils With Cavities. *Journal of Engineering*, 13(01), 1166–1186. doi:10.31026/j.eng.2007.01.03.
- [5] Jebur, M. M., Ahmed, M. D., & Karkush, M. O. (2020). Numerical Analysis of Under-Reamed Pile Subjected to Dynamic Loading in Sandy Soil. *IOP Conference Series: Materials Science and Engineering*, 671(1), 12084. doi:10.1088/1757-899X/671/1/012084.
- [6] Rashid Al-Qayssi, M., Faik Al-Wakel, S., & Khairalla Abdalazez Kando, A. (2018). Experimental Study of Model Piled Raft Foundation Embedded Within Partially Saturated Cohesionless Soils. *Journal of Engineering and Sustainable Development*, 2018(03), 62–75. doi:10.31272/jeasd.2018.3.6.
- [7] Mahmood, M. R., Al-Wakel, S. F. A., & Hani, A. A. (2017). Experimental and Numerical Analysis of Piled Raft Foundation Embedded within Partially Saturated Soil. *Engineering and Technology Journal*, 35(2A), 97–105. doi:10.30684/etj.35.2a.1.
- [8] Milovic, D. M., & Todorovic, T. (1985). Stresses and Displacements in an Anisotropic Soil Produced By a Ring Foundation. *International Journal of Rock Mechanics and Mining Sciences & Geomechanics Abstracts*, 24(3), 821–827. doi:10.1016/0148-9062(87)90757-1.
- [9] Broms, B. B. (1963). Allowable Bearing Capacity of Initially Bent Piles. *Journal of the Soil Mechanics and Foundations Division*, 89(5), 73–90. doi:10.1061/jsfeaq.0000559.
- [10] Oloo, S. Y., Fredlund, D. G., & Gan, J. K. M. (1997). Bearing capacity of unpaved roads. *Canadian Geotechnical Journal*, 34(3), 398–407. doi:10.1139/t96-084.
- [11] Vanapalli, S. K., & Mohamed, F. M. O. (2007). Bearing Capacity of Model Footings in Unsaturated Soils. *Experimental Unsaturated Soil Mechanics*, 483–493. doi:10.1007/3-540-69873-6_48.
- [12] Oh, W. T., Vanapalli, S. K., & Puppala, A. J. (2009). Semi-empirical model for the prediction of modulus of elasticity for unsaturated soils. *Canadian Geotechnical Journal*, 46(8), 903–914. doi:10.1139/T09-030.
- [13] Taylan, Z. N., & Vanapalli, S. K. (2012). Estimation of the Shaft Capacity of Single Piles Using the Conventional and Modified β Method. *Unsaturated Soils: Research and Applications*, 255–262. doi:10.1007/978-3-642-31343-1_32.
- [14] ASTM D854-23. (2023). Standard Test Methods for Specific Gravity of Soil Solids by the Water Displacement Method. ASTM International, Pennsylvania, United States. doi:10.1520/D0854-23.
- [15] Ravindran, S., & Gratchev, I. (2022). Effect of Water Content on Apparent Cohesion of Soils from Landslide Sites. *Geotechnics*, 2(2), 385–394. doi:10.3390/geotechnics2020017.
- [16] ASTM D4253. (2019). Standard Test Methods for Maximum Index Density and Unit Weight of Soils Using a Vibratory Table. ASTM International, Pennsylvania, United States. doi:10.1520/D4253-16E01.
- [17] ASTM D4254-16. (2016). Standard Test Methods for Minimum Index Density and Unit Weight of Soils and Calculation of Relative Density. ASTM International, Pennsylvania, United States. doi:10.1520/D4254-16.
- [18] ASTM D3080-04. (2011). Standard Test Method for Direct Shear Test of Soils under Consolidated Drained Conditions ASTM International, Pennsylvania, United States. doi:10.1520/D3080-04.
- [19] Ridley, A. (2015). Soil suction — what it is and how to successfully measure it. *Proceedings of the Ninth Symposium on Field Measurements in Geomechanics*, 27–46. doi:10.36487/acg_rep/1508_0.2_ridley.
- [20] Li, X. (2008). Laboratory studies on the bearing capacity of unsaturated sands. PhD Thesis, University of Ottawa, Ottawa, Canada.
- [21] Vanapalli, S. K., Sun, R., & Li, X. (2011). Bearing capacity of an unsaturated sand from model footing tests. *Unsaturated Soils - Proceedings of the 5th International Conference on Unsaturated Soils*, 2, 1217–1222. doi:10.1201/b10526-189.
- [22] Fredlund, D. G., Sheng, D., & Zhao, J. (2011). Estimation of soil suction from the soil-water characteristic curve. *Canadian Geotechnical Journal*, 48(2), 186–198. doi:10.1139/T10-060.
- [23] Fredlund, D. G., & Xing, A. (1994). Equations for the soil-water characteristic curve. *Canadian Geotechnical Journal*, 31(4), 521–532. doi:10.1139/t94-061.

- [24] van Genuchten, M. T. (1980). A Closed- form Equation for Predicting the Hydraulic Conductivity of Unsaturated Soils. *Soil Science Society of America Journal*, 44(5), 892–898. doi:10.2136/sssaj1980.03615995004400050002x.
- [25] Leong, E. C., & Rahardjo, H. (1997). Permeability Functions for Unsaturated Soils. *Journal of Geotechnical and Geoenvironmental Engineering*, 123(12), 1118–1126. doi:10.1061/(asce)1090-0241(1997)123:12(1118).
- [26] Terzaghi, K. (1943). *Theoretical Soil Mechanics*. John Wiley & Sons, Hoboken, United States. doi:10.1002/9780470172766.
- [27] Fattah, M. Y., Ahmed, M. D., & Mohammed, H. A. (2023). Behavior of Partially Saturated Cohesive Soil under Strip Footing. *Journal of Engineering*, 19(3), 298–311. doi:10.31026/j.eng.2013.03.02.
- [28] Abood, A. S., Fattah, M. Y., & Al-Adili, A. (2023). Assessment of shear strength characteristics of the unsaturated gypseous soil at various saturation degrees. *Cogent Engineering*, 10(2), 2283303. doi:10.1080/23311916.2023.2283303.
- [29] Fredlund, D. G., Rahardjo, H., & Fredlund, M. D. (2012). *Unsaturated Soil Mechanics in Engineering Practice*. John Wiley & Sons, Hoboken, United States. doi:10.1002/9781118280492.
- [30] Ibrahim, A. A., & Karkush, M. O. (2023). The Efficiency of Belled Piles in Multi-Layers Soils Subjected to Axial Compression and Pullout Loads: Review. *Journal of Engineering*, 29(09), 166–183. doi:10.31026/j.eng.2023.09.12.
- [31] Mahmood, M. R., Salim, N. M., & Al-Gezzy, A. A. (2021). Effect of Different Soil Saturation Conditions on the Ultimate Uplift Resistance of Helical Pile Model. *E3S Web of Conferences*, 318, 01012. doi:10.1051/e3sconf/202131801012.